

SCIENTIFIC REPORTS

OPEN

Understanding the Mechanism of Action of the Anti-Dandruff Agent Zinc Pyrithione against *Malassezia restricta*

Minji Park¹, Yong-Joon Cho², Yang Won Lee^{3,4} & Won Hee Jung¹

Dandruff is known to be associated with *Malassezia restricta*. Zinc pyrithione (ZPT) has been used as an ingredient in anti-dandruff treatments. The mechanism of ZPT has been investigated in several studies; however, a non-pathogenic model yeast, such as *Saccharomyces cerevisiae* was most often used. The aim of the present study was to understand how ZPT inhibits the growth of *M. restricta*. We analyzed the cellular metal content and transcriptome profile of ZPT-treated *M. restricta* cells and found that ZPT treatment dramatically increased cellular zinc levels, along with a small increase in cellular copper levels. Moreover, our transcriptome analysis showed that ZPT inhibits Fe-S cluster synthesis in *M. restricta*. We also observed that ZPT treatment significantly reduced the expression of lipases, whose activities contribute to the survival and virulence of *M. restricta* on human skin. Therefore, the results of our study suggest that at least three inhibitory mechanisms are associated with the action of ZPT against *M. restricta*: (i) an increase in cellular zinc levels, (ii) inhibition of mitochondrial function, and (iii) a decrease in lipase expression.

Dandruff is a common scalp condition associated with abnormal scalp flaking. Half of the adult human population is affected by the condition at some time in their lives¹. In general, dandruff is ascribed to three etiological factors, *Malassezia* yeast, sebaceous secretions, and individual susceptibility². Among these, *Malassezia* yeast has long been considered the main cause of dandruff; this idea is supported by improvement in dandruff, accompanied by a reduction in the number of the yeast cells on the scalp, following treatment with a shampoo containing an antifungal agent^{3–5}. A total of 17 different *Malassezia* species have been identified, and, among them, *M. restricta* is the dominant species on human skin^{6–10}. Moreover, recent large-scale sequencing analyses have indicated increased presence of *M. restricta* on scalps with dandruff compared to that on healthy scalps, suggesting an association between the fungus and dandruff^{8,11,12}. The studies have suggested that lipases secreted from *Malassezia* contribute to the development of dandruff and led to the hypothesis that these enzymes hydrolyze sebum triglycerides and help the yeast cells take up saturated fatty acids to generate energy. The accumulation of excess unsaturated fatty acids, such as oleic acid, on the skin causes skin irritation in patients suffering from dandruff^{2,13}.

Zinc pyrithione is a derivative of pyrithione (1-hydroxy-2-pyridinethione), which is synthesized from the antimicrobial metabolite ‘aspergillilic acid’ of *Aspergillus flavus*^{14–17}. A number of shampoos and rinse-off products containing 0.3–2% ZPT have been used extensively over the counter to treat dandruff¹⁸. Although the use of ZPT as an antidandruff agent is widespread, its mechanism of action against *Malassezia*, and *M. restricta* in particular, is still unclear; only physiological observations of *Malassezia* growth inhibition by ZPT have been reported^{19,20}. The mechanism of action of ZPT has been characterized using different model fungal organisms, rather than *M. restricta*. Ermolayeva and Sanders²¹ used *Neurospora crassa* and suggested that ZPT leads to membrane depolarization either directly or indirectly, thereby, inhibiting proton pump-mediated membrane transport. They suggested that this inhibition might be caused solely by pyrithione, because zinc salt is believed to dissociate after ZPT is transported into the cytosol, and that pyrithione alone acted in this manner^{21,22}. However, membrane

¹Department of Systems Biotechnology, Chung-Ang University, Anseong, 17546, Korea. ²Korea Polar Research Institute, Incheon, 21990, Korea. ³Department of Dermatology, School of Medicine, Konkuk University, Seoul, 05029, Korea. ⁴Research Institute of Medicine, Konkuk University, Seoul, 05029, Korea. Correspondence and requests for materials should be addressed to Y.W.L. (email: 20050078@kuh.ac.kr) or W.H.J. (email: whjung@cau.ac.kr)

Received: 12 April 2018

Accepted: 1 August 2018

Published online: 14 August 2018

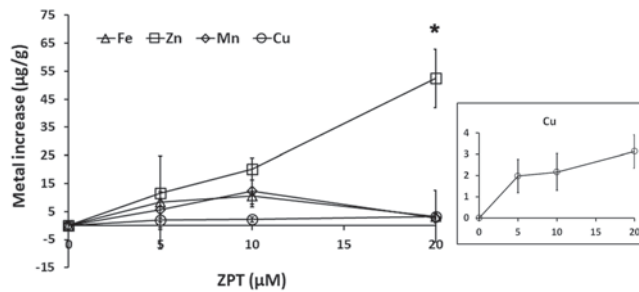


Figure 1. Metal content of ZPT-treated *M. restricta* cells. The iron, copper, zinc, and manganese levels in *M. restricta* KCTC 27527 cells grown in media containing different concentrations of ZPT were determined by ICP analysis. Values represent the average from three independent experiments with standard deviations (* $p < 0.005$). Changes in copper levels are shown separately.

depolarization occurs at a significantly higher concentration of pyrithione, which is beyond the inhibitory concentration for the fungi²³; therefore, it is difficult to assert that the mechanism of action of ZPT on fungi involves membrane depolarization.

Yasokawa *et al.*²⁴ analyzed the transcriptome of *Saccharomyces cerevisiae* cells treated with ZPT and found that the compound upregulates the expression of genes required for iron transport. These results suggested that ZPT induces iron starvation in the yeast cells. Furthermore, they observed that the addition of iron restored the growth of *S. cerevisiae* cells in medium containing ZPT, supporting the idea that the compound induces iron deficiency in the yeast. In contrast, another study by Reeder *et al.*²⁵ showed that iron levels in ZPT-treated *S. cerevisiae* cells were not changed, although they observed an upregulation of expression of Fet3, a ferroxidase in the high-affinity reductive iron transport system, which suggested that iron starvation might not be a direct cause of ZPT toxicity. Instead, Reeder *et al.*²⁵ found that cellular copper levels were increased on ZPT treatment and observed a downregulation of *CTR1*, a high-affinity copper transporter in the plasma membrane. To confirm that increased cellular copper levels are one of the main causes of growth inhibition by ZPT, a *S. cerevisiae* haploid gene deletion library was screened against ZPT. Deletion mutants that were growth inhibited upon ZPT treatment included a mutant lacking *ACE1*, which encodes a transcription factor responsible for detoxification of high cellular copper levels, a finding of which supports the idea that ZPT treatment causes copper toxicity in yeast cells. Moreover, a number of deletion mutants that lack genes involved in iron-sulfur cluster (Fe-S) assembly in mitochondria showed significant growth defects following ZPT treatment. These results suggested that, in addition to copper toxicity, copper-mediated inactivation of Fe-S cluster assembly in mitochondria also contributes to growth inhibition by ZPT, at least in *S. cerevisiae*.

Although previous studies have suggested possible mechanisms of action of ZPT against model fungal organisms, they have not clearly explained how ZPT inhibits the growth of *Malassezia*, which is phylogenetically distant. Therefore, in this study, we attempted to understand the mechanism of action of ZPT against *M. restricta*, using biochemical and transcriptome analyses and found that ZPT mainly triggered zinc toxicity and mitochondrial dysfunction. Furthermore, our data suggested that ZPT decreases expression of lipases, which may play an important role in survival of the *M. restricta* on the surfaces of scalps of patients with dandruff^{3,26,27}. To our knowledge, this is the first comprehensive study to directly investigate the mechanism of action of ZPT against *M. restricta*.

Results

ZPT treatment led to an increase in cellular zinc levels in *M. restricta*. ZPT is a well-known zinc ionophore that has antifungal activity, and several studies using model fungi have indicated that alteration of cellular metal content is one of the main antifungal mechanisms of action of the compound. Examples include an increase in cellular copper levels in ZPT-treated *S. cerevisiae*, as mentioned previously. We, therefore, investigated how ZPT treatment altered cellular levels of essential metals, such as copper, zinc, manganese, and iron. The metal content of ZPT-treated *S. cerevisiae* cells was measured in parallel with inductively coupled plasma-atomic emission spectroscopy (ICP-AES) to replicate data previously reported by Reeder *et al.*²⁵. The results were similar to what was previously observed (see Supplementary Table S1), confirming that ZPT increases cellular copper levels in *S. cerevisiae*. Furthermore, the results indicated that our method to determine cellular metal levels was reliable.

Subsequently, cellular levels of essential metals in *M. restricta* cells grown in the presence of ZPT were determined by the same method used to investigate whether ZPT altered cellular metal levels in the fungus, and the results showed that, among the essential metals, cellular zinc levels were significantly and dose-dependently increased in cells grown in the presence of ZPT. However, unlike *S. cerevisiae*, only a small increase in copper levels was observed in cells grown in the presence of ZPT compared to that in cells grown in the absence of the compound, and no change in iron or manganese levels was detected (Fig. 1). These data suggest that the mechanism by which ZPT affects the metal content in *M. restricta* is different from that in *S. cerevisiae*, and that ZPT mainly increased zinc levels along with small increase of copper levels in *M. restricta* cells, unlike what was observed in *S. cerevisiae* cells.

N,N,N',N'-Tetrakis(2-pyridylmethyl)ethylenediamine (TPEN) is a high-affinity membrane permeable zinc chelator that has been used to investigate the effects of cellular zinc levels in multiple organisms, including fungi. Previous studies have suggested that ZPT dissociates into pyrithione and zinc salt once it is transported into the

	MIC (μM)
ZPT	2.5–5
ZPT + TPEN 25 μM	5–10
ZPT + TPEN 50 μM	10
ZPT + BCS 50 μM	2.5–5
ZPT + BCS 100 μM	2.5–5

Table 1. *In vitro* antifungal susceptibilities of *M. restricta* to ZPT with TPEN or BCS and pyrithione.

ZPT treatment	The number of up-regulated genes					The number of down-regulated genes					Total
	2-Fold	3-Fold	4-Fold	>5-Fold	Total	2-Fold	3-Fold	4-Fold	>5-Fold	Total	
5 μM	14	5			19	64	10	1	1	76	95
10 μM	152	19	8	1	180	204	54	24	28	310	490
20 μM	221	50	10	13	294	267	80	29	54	430	724

Table 2. Number of genes regulated by ZPT treatment compared to no treatment.

cytosol^{21,22}. Therefore, we hypothesized that TPEN would chelate hyperaccumulated cellular zinc in the cytosol of *M. restricta* cells grown in the presence of ZPT, and that the inhibitory activity of ZPT against *M. restricta* would be reduced if TPEN and ZPT were added together. To test this hypothesis, we determined the minimal inhibitory concentration (MIC) of ZPT in the presence or absence of TPEN and found that the MIC of ZPT was reduced when it was added with TPEN (Table 1). These data confirmed our finding that ZPT increases cellular zinc levels in *M. restricta*. Additionally, we observed that ZPT caused swelling of *M. restricta* cells, and this abnormal morphological characteristic was restored by TPEN, but not by BCS. These data further support our findings (Supplementary Fig. S1). However, we should note that the addition of TPEN did not completely eliminate the antifungal activity of ZPT. These results imply that an increase in cellular zinc levels is not the only mechanism of antifungal action, but that pyrithione, which is dissociated from ZPT, might also inhibit *M. restricta*. Bathocuproine disulfonate (BCS) is a copper chelator, and its effect on the antifungal activity of ZPT against *M. restricta* was also tested. Unlike TPEN, the addition of BCS did not alter the MIC of ZPT, suggesting that the change in cellular copper levels was minimal.

ZPT triggered a large change in the transcriptome and interfered with mitochondrial functions in *M. restricta*.

To understand the mechanism of ZPT action in more detail, we investigated how ZPT affects the transcriptome of *M. restricta* cells, using the recently determined genome sequence of *M. restricta* KCTC 27527²⁶. Transcriptomes of *M. restricta* cells grown in the presence of 5, 10, and 20 μM ZPT were analyzed by RNA sequencing (see Methods) and compared with those of cells grown in the absence of the compound. The minimum ZPT concentration of 5 μM was selected based on the MIC of the compound against *M. restricta*, and 2-fold increases in ZPT concentrations up to 20 μM were used to analyze the dose dependence of differentially expressed genes. The results of the transcriptome analysis showed that many genes were differentially expressed: 95, 490, and 724 genes were up or downregulated more than 2-fold in the cells grown in the presence of 5, 10, and 20 μM of ZPT, respectively, compared with the cells grown in medium without ZPT (Table 2 and Supplementary Table S2). Differential expression of few key genes were selected and validated by quantitative real time PCR (qRT-PCR; Supplementary Table S3).

We hypothesized that the genes that were directly affected by ZPT would show differential and dose-dependent expression in *M. restricta* cells grown in the media containing 5, 10, and 20 μM of ZPT. Applying highly stringent selection criteria, we found that, among the genes that were differentially expressed more than 2-fold, 12 and 40 genes were up and downregulated, respectively, in a dose-dependent manner in the cells grown in media containing different concentrations of ZPT. Moreover, we found that mitochondrial function might be one of the major targets of ZPT, because genes encoding mitochondrial proteins were the most enriched among the genes showing differential dose-dependent regulation (Fig. 2) such that 3 encoding mitochondrial proteins were upregulated while 8 were downregulated. In particular, the expression of MRES_05505 (succinate dehydrogenase), MRES_03900 (citrate synthase), MRES_00405 (ATP synthase subunit), and MRES_00105 (ATP synthase subunit), which are components of the tricarboxylic acid (TCA) cycle and electron transport chain, was downregulated significantly and dose-dependently.

In a previous genome analysis, we identified two genes, MRES_16605 and MRES_08815 that are homologs of *ACO1* and *ACO2*, respectively, encoding aconitase in *S. cerevisiae*²⁶. The current transcriptome analysis showed that *ACO1* homolog MRES_16605 was significantly downregulated in *M. restricta* cells grown in the presence of 5 and 10 μM ZPT, although the gene was not included in the list of dose-dependently regulated genes, because it was downregulated slightly less in the cells grown in medium containing 20 μM of ZPT. However, we confirmed reduced activity of aconitase in ZPT-treated *M. restricta* cells (Fig. 3). In agreement with this reduction in aconitase activity, the results of our transcriptome analysis showed that ZPT treatment upregulated a number of genes related to Fe-S cluster biosynthesis in *M. restricta* (Table 3). MRES_02625, MRES_04375, MRES_14620, and MRES_16875 were predicted to be required for Fe-S cluster assembly and were upregulated in a concentration-dependent manner in ZPT-treated *M. restricta* cells. We reasoned that upregulation of these

Gene	Annotation	Localization	5 μ M	10 μ M	20 μ M
MRES_09910	hypothetical protein	Cytoplasm	2.31	4.57	6.62
MRES_17040	permease for cytosine/purines, uracil, thiamine, allantoin	Unknown	2.60	3.97	6.51
MRES_05530	angio-associated migratory cell protein (contains WD40 repeats)	Nucleus	2.05	3.15	3.15
MRES_11225	hypothetical protein	Unknown	2.12	4.93	6.04
MRES_16765	predicted transporter (major facilitator superfamily)	Plasma membrane	2.23	2.50	2.79
MRES_16365	hypothetical protein	Endoplasmic reticulum	3.33	4.63	5.40
MRES_03565	ubiquitin family protein	Unknown	2.41	4.47	5.26
MRES_12755	flavin-containing monooxygenase	Cytoplasm	3.56	3.80	4.55
MRES_03330	U1-like Zn-finger-containing protein, role in RNA processing/splicing	Nucleus	2.10	3.58	3.64
MRES_09125	hypothetical protein	Mitochondria	3.25	5.48	6.30
MRES_10495	peptidyl-tRNA hydrolase	Mitochondria	2.10	4.19	5.97
MRES_10905	mitochondrial carrier protein	Mitochondria	2.34	2.71	3.49
MRES_05505	succinate dehydrogenase (ubiquinone)	Mitochondria	0.32	0.22	0.19
MRES_11930	mitochondrial carrier protein	Mitochondria	0.48	0.17	0.06
MRES_08605	manganese superoxide dismutase	Mitochondria	0.41	0.13	0.07
MRES_00495	phosphoenolpyruvate carboxykinase (ATP)	Mitochondria	0.37	0.23	0.22
MRES_02180	Inorganic diphosphatase	Mitochondria	0.42	0.25	0.22
MRES_03900	citrate synthase	Mitochondria	0.44	0.23	0.27
MRES_00405	mitochondrial F1F0-ATP synthase	Mitochondria	0.49	0.23	0.21
MRES_00105	F0F1-type ATP synthase, gamma subunit	Mitochondria	0.48	0.29	0.28
MRES_03205	Lipase (class 3)	Extracellular	0.49	0.17	0.16
MRES_04670	secretory lipase (family LIP)	Extracellular	0.36	0.10	0.06
MRES_16530	secretory lipase (family LIP)	Extracellular	0.39	0.19	0.14
MRES_03670	secretory lipase (family LIP)	Extracellular	0.35	0.15	0.14
MRES_05740	hypothetical protein	Unknown	0.46	0.13	0.07
MRES_11310	ferric reductase	Plasma membrane	0.19	0.09	0.08
MRES_03975	histone H2B	Nucleus	0.27	0.17	0.09
MRES_02860	hypothetical protein	Plasma membrane	0.44	0.17	0.10
MRES_00975	cyclin	Nucleus	0.33	0.11	0.11
MRES_14425	hypothetical protein	Cytoplasm	0.37	0.14	0.11
MRES_04840	S-adenosylhomocysteine hydrolase	Cytoplasm	0.32	0.12	0.12
MRES_14700	S-adenosylmethionine synthetase	Cytoplasm	0.42	0.15	0.12
MRES_15340	hypothetical protein	Unknown	0.38	0.13	0.12
MRES_07350	hypothetical protein	Unknown	0.45	0.16	0.13
MRES_06495	aspartyl protease	Extracellular	0.36	0.16	0.13
MRES_17090	polyC-binding protein α CP-1 and related KH domain protein	Cytoplasm	0.33	0.18	0.14
MRES_02875	COP9 signalosome, subunit CSN2	Cytoplasm	0.47	0.16	0.15
MRES_05025	glycosylhydrolase	Nucleus	0.38	0.20	0.16
MRES_05765	hypothetical protein	Unknown	0.25	0.18	0.16
MRES_17845	aspartyl protease	Extracellular	0.36	0.21	0.18
MRES_02050	hypothetical protein	Cytoplasm	0.38	0.19	0.18
MRES_00005	aspartyl protease	Extracellular	0.33	0.22	0.20
MRES_09430	cobalamin-independent synthase	Cytoplasm	0.42	0.24	0.20
MRES_04160	hypothetical protein	Nucleus	0.45	0.29	0.23
MRES_17785	hypothetical protein	Unknown	0.41	0.26	0.25
MRES_02125	TEF-1 and related transcription factor, TEAD family	Nucleus	0.47	0.30	0.27
MRES_11550	hypothetical protein	Extracellular	0.39	0.31	0.27
MRES_00970	predicted BBOX Zn-finger protein	Nucleus	0.48	0.32	0.29
MRES_13415	glucan 1,3-beta-glucosidase	Plasma membrane	0.36	0.33	0.30
MRES_10595	Ctr copper transporter family	Unknown	0.47	0.33	0.33
MRES_06755	hypothetical protein	Cytoplasm	0.46	0.41	0.38
MRES_04905	hypothetical protein	Unknown	0.46	0.41	0.40



Figure 2. List of differentially expressed genes in ZPT-treated *M. restricta* cells. Genes that were more than 2-fold differentially up or downregulated in a dose-dependent manner in ZPT-treated *M. restricta* cells are shown. The values indicate the ratio of TMM of the corresponding gene in *M. restricta* cells grown in media containing different concentrations of ZPT vs. cells grown in medium without the compound.

genes occurred in the ZPT-treated cells to compensate for the inhibition of Fe-S cluster biosynthesis by ZPT. We should also note that these genes required for Fe-S biosynthesis were not included in the Fig. 2 of differentially expressed genes, because the changes in their expression in cells treated with 5 μ M of ZPT were less than 2-fold.

In addition to alterations in the expression of genes required for Fe-S cluster synthesis in mitochondria, MRES_08605, which encodes the homolog of *S. cerevisiae* Sod2, a manganese dependent mitochondrial superoxide dismutase, was found to be one of the most strongly dose-dependently downregulated genes in ZPT-treated *M. restricta* cells. It was shown that, in *S. cerevisiae*, SOD2 transcription is significantly reduced with a decrease in heme synthesis, which occurs mainly within the mitochondria^{28,29}. We, therefore, hypothesized that increased

Gene name	Annotation	Fold (+ZPT/–ZPT)		
		5 μ M	10 μ M	20 μ M
MRES_02625	Cytosolic Fe-S cluster assembly factor Nar1	1.81	3.03	3.47
MRES_04375	Fe-S cluster assembly protein Dre2	1.36	2.41	3.35
MRES_14620	Fe-S cluster assembly scaffold protein IscU	1.98	4.18	6.38
MRES_16875	Fe-S cluster scaffold homolog Nfu1	1.42	2.48	2.70

Table 3. Expression of Fe-S cluster synthesis-related genes following ZPT treatment.

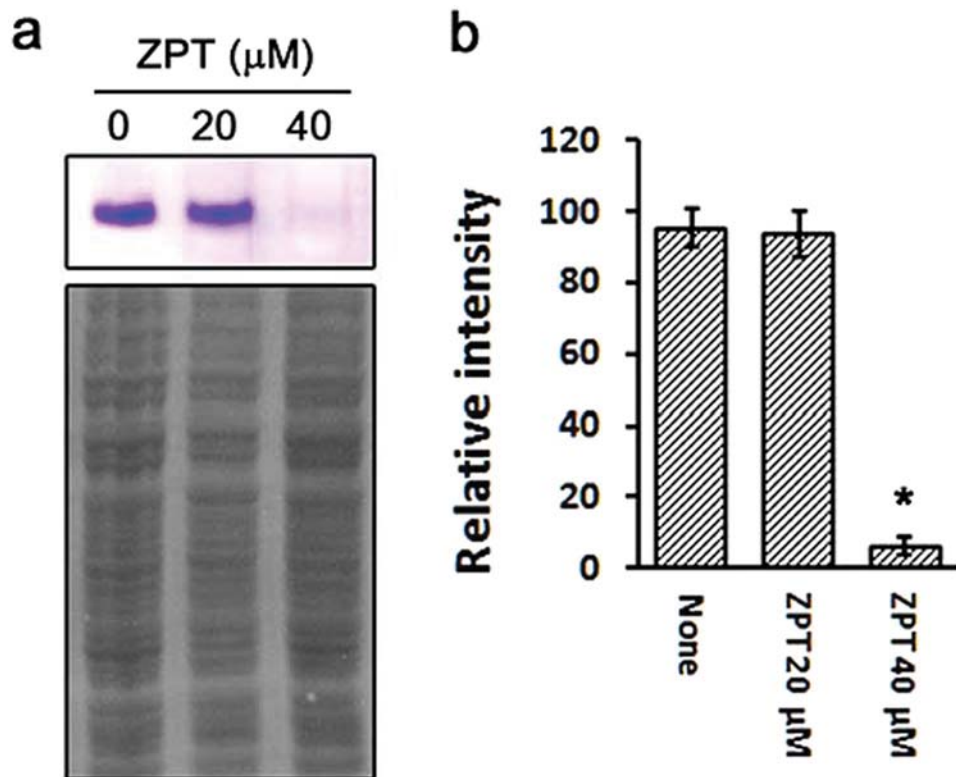


Figure 3. Activity of aconitase in ZPT-treated *M. restricta* cells. (a) Activity of aconitase in *M. restricta* KCTC 27527 cells grown in media containing 0, 20, or 40 μ M of ZPT was assessed by gel-based aconitase assay (upper panel). As a loading control, the same samples were resolved on a polyacrylamide gel, transferred to nitrocellulose membranes, and stained with CPTA (lower panel). (b) The intensities of bands were quantified in ImageJ and compared. Values represent the average from three independent experiments with standard deviations (* $p < 0.0001$).

zinc accumulation in ZPT-treated *M. restricta* cells disrupted mitochondrial heme biogenesis and led to down-regulation of *SOD2*. Taken together, our data suggested that ZPT interferes substantially with mitochondrial functions in *M. restricta* cells.

ZPT altered the expression of genes involved in zinc and copper uptake in *M. restricta*. Altered cellular metal content in ZPT-treated *M. restricta* led us to investigate the differential expression of genes involved in zinc and copper transport. We first searched the genome of *M. restricta* for homologs of *S. cerevisiae* genes involved in transport of metals and found a few unique characteristics of metal transport systems in *M. restricta*. These include the presence of only a single copper transporter on the plasma membrane of *M. restricta*, whereas other fungi have at least two paralogous genes (*CTR1* and *CTR3* in *S. cerevisiae*^{30,31} and *CTR1* and *CTR4* in *Cryptococcus neoformans*, for example^{32,33}). In addition, no vacuolar copper transporter, a homolog of *S. cerevisiae* *CTR2*³⁴, was identified in the genome of *M. restricta*. In contrast, almost all homologs of zinc transporters, including two zinc transporters on the plasma membrane, were identified in the genome of *M. restricta* (Table 4). These findings suggested that *M. restricta* utilizes the conserved zinc transport system, with a limited number of genetic components used for copper transport in the fungus.

We next analyzed the transcriptome data to determine expression patterns of genes involved in the transport of metals in ZPT-treated *M. restricta* cells. As shown in Table 4, the gene MRES_04925, which is a homolog of

	<i>S. cerevisiae</i>	<i>C. albicans</i>	<i>C. neoformans</i>	<i>M. restricta</i>	Annotation	Fold (+ZPT/–ZPT)		
						5 μ M	10 μ M	20 μ M
Cu transporter	<i>CTR1</i>	<i>CTR1</i>	CNAG_07701 (<i>CTR1</i>)	No hit				
	<i>CTR2</i>	<i>CTR2</i>	CNAG_01872 (<i>CTR2</i>)	No hit				
	<i>CTR3</i>		CNAG_00979 (<i>CTR4</i>)	MRES_10595	Ctr copper transporter family	0.47	0.33	0.33
Zn transporter	<i>ZRT1</i>		CNAG_00895 (<i>ZIP1</i>)	MRES_03690/ MRES_03695	ZIP zinc transporter, High-affinity zinc transport protein, Regulates intracellular zinc levels	0.60/1.11	0.64/0.87	0.65/0.65
	<i>ZRT2</i>	<i>ZRT1</i> <i>ZRT2</i>	CNAG_03398					
	<i>ZRT3</i>	<i>C2_02180W_A</i>	CNAG_02221	MRES_11910	ZIP zinc transporter, May act as a zinc-influx transporter	1.49	1.61	1.32
	<i>ZRC1</i>		CNAG_02806	MRES_04925	Region of a membrane-bound protein predicted to be embedded in the membrane, Zn ²⁺ transporter Znt1 and related Cd ²⁺ /Zn ²⁺ transporters (cation diffusion facilitator superfamily)	1.53	2.87	3.14
	<i>YKE4</i>		CNAG_02993	No hit				

Table 4. Expression of Cu and Zn transporter genes following ZPT treatment.

S. cerevisiae *ZRC1* and *COT1*, was upregulated in cells grown in the presence of 10 and 20 μ M of ZPT. We should note that special attention was paid to MRES_04925 because of its possible function in zinc transport and homeostasis, although the gene was not included in the list of genes expressed differentially and dose-dependently. However, dose-dependent upregulation of the gene was observed in cells grown in the presence of 10 and 20 μ M ZPT. *Zrc1* and *Cot1* are vacuolar zinc importers in *S. cerevisiae* that are responsible for zinc transport into vacuoles when intracellular zinc concentrations in a cell increase³⁵. Increased expression of the *ZRC1* and *COT1* homolog in ZPT-treated *M. restricta* cells agreed with our findings of increased cellular zinc levels. We should also note that we observed a small reduction in the expression of MRES_03690 and MRES_03695, the homologs of *S. cerevisiae* *ZRT1* and *ZRT2*, which are plasma membrane transporters required for zinc uptake. The gene MRES_10595, the homolog of *S. cerevisiae* *CTR3*, was downregulated in ZPT-treated *M. restricta* cells. This data agreed with our findings in Fig. 1 showing slightly increased cellular copper levels in ZPT-treated *M. restricta* cells and implied that copper accumulation might also contribute inhibitory mechanism of ZPT at least partly.

ZPT inhibits the expression of *M. restricta* lipase. Another group of genes that showed a significant differential response to ZPT was lipases. We previously identified 12 lipase genes in the genome of *M. restricta* KCTC 27527²⁶. Among them, MRES_03205 (*MrLIP1*), MRES_03670 (*MrLIP5*), MRES_04670 (*MrLIP3*), and MRES_16530 were downregulated more than 2-fold in a dose-dependent manner in response to ZPT treatment. Putative lipase-encoding genes, MRES_15190 and MRES_15265 (*MrLIP2*), were also downregulated in a dose-dependent manner, but slightly less than 2-fold with 5 and 10 μ M ZPT. In total, the expression of 6 out of 12 lipases was downregulated in ZPT-treated cells (Fig. 4a). We paid special attention to the downregulation of lipase genes, because these enzymes are believed to play key roles in the pathogenesis of *Malassezia* species^{2,26,27,36}. Among them, *MrLIP5* was of particular interest, because it was identified as a major lipase-encoding gene and the most frequently expressed gene in the scalps of patients with dandruff²⁶. To confirm downregulation of lipases by ZPT, we performed a western blot analysis using antisera specific to MrLip1 and MrLip5 and found that the decreased transcript levels observed in our transcriptome analysis reflected significantly reduced protein levels (Fig. 4b,c). The results of the western blot analysis also suggested that reduced expression of lipases was not a response to an increase in zinc or copper in the medium. Moreover, downregulation of the expression of lipases, MrLip1 and MrLip5 in particular, by ZPT has been observed in other clinical isolates of *M. restricta*, eliminating the possibility of a strain-specific inhibitory effect of ZPT on lipase expression (Fig. 4d). These results indicated that ZPT had an inhibitory effect on lipase expression across various clinical strains of *M. restricta*, suggesting that this is a general mechanism by which the compound limits *M. restricta*.

Discussion

In the present study, we aimed to understand the mechanism of action of ZPT against *M. restricta* and found that ZPT treatment significantly increased cellular zinc levels in the fungus along with a small increase of cellular copper levels. A reduction in the antifungal activity of ZPT on *M. restricta* by TPEN, an cellular zinc chelator, but not by BCS, a copper chelator, supports our observation that ZPT treatment mainly causes increase in cellular zinc levels. These results were different from what was found in a previous study with *S. cerevisiae*, which showed that the addition of BCS rescued the growth of fungal cells treated with ZPT²⁵ and suggested that the mechanism of action of ZPT against *M. restricta* is different from that against *S. cerevisiae*. In *S. cerevisiae*, two plasma membrane proteins, Ctr1 and Ctr3, are responsible for high-affinity copper uptake, and Ctr2 is involved in copper export through the vacuolar membrane. The previous study showed that ZPT triggered a 0.08–0.23-fold decrease in *CTR1*, supporting the idea that cellular copper levels are increased in response to the compound in *S. cerevisiae*. However, we discovered that *M. restricta* lacks homologs of *S. cerevisiae* Ctr1 and Ctr2. Instead, *M. restricta* may utilize a single copper transporter, a homolog of *S. cerevisiae* Ctr3, to transport copper through the

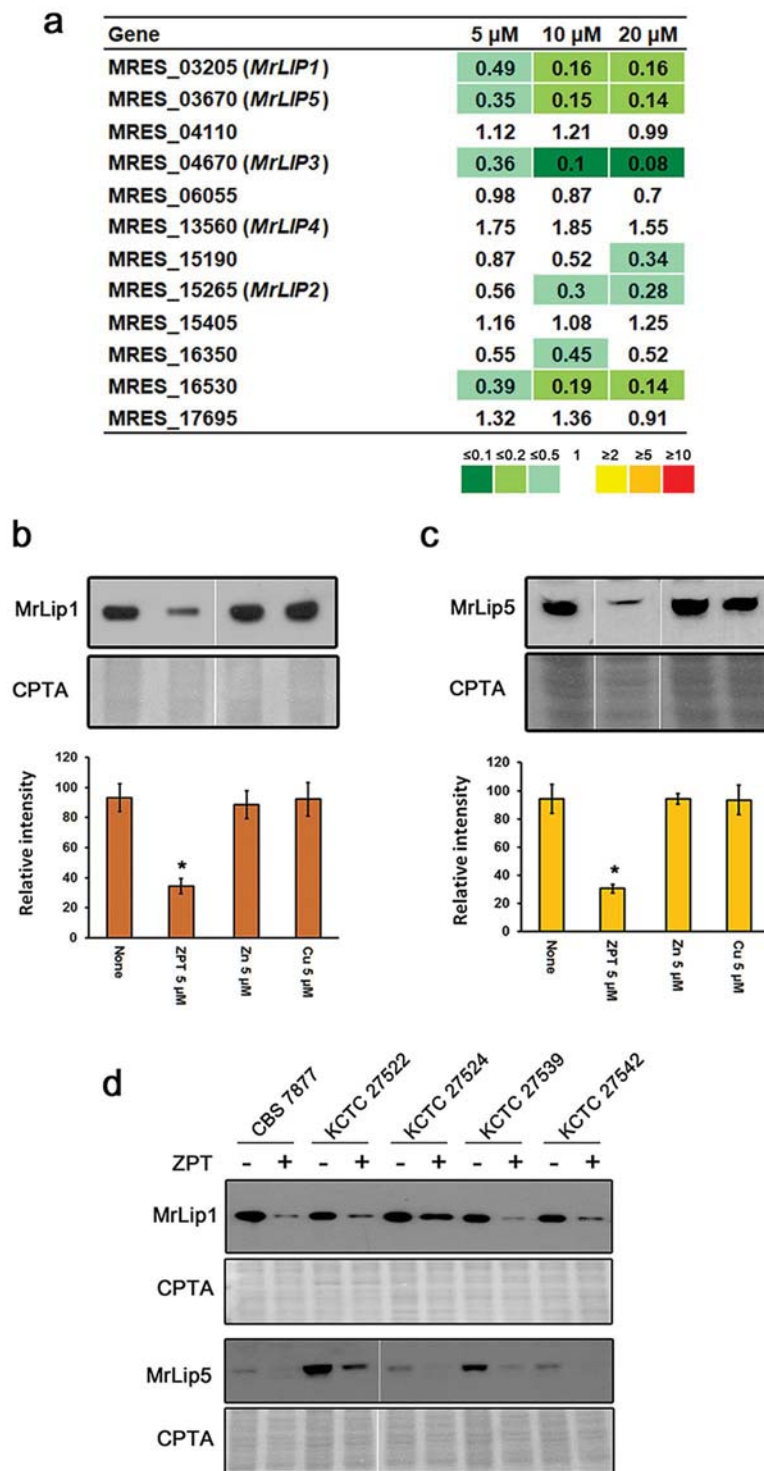


Figure 4. Inhibition of the expression of *M. restricta* lipases by ZPT. **(a)** Differential expression of 12 lipase genes in ZPT-treated *M. restricta* KCTC 27527 cells. The values indicate the ratio of TMM of the corresponding genes in *M. restricta* cells grown in media containing different concentrations of ZPT vs. cells in grown in medium without the compound. **(b)** Inhibition of MrLip1 expression in *M. restricta* cells grown in media containing 5 μ M of ZPT, ZnCl₂ or CuCl₂ (upper panel). Relative intensities of expression were quantified in ImageJ and compared (lower panel). Values represent the average from three independent experiments with standard deviations (**p* < 0.0001). The cropped blots are used in the figure, and the full-length blots are presented in Supplementary Fig. S2. **(c)** Inhibition of MrLip5 expression in *M. restricta* cells grown in media containing 5 μ M of ZPT, ZnCl₂ or CuCl₂ (upper panel). Relative intensities of expression were quantified in ImageJ and compared (lower panel). Values represent the average from three independent experiments with standard deviations (**p* < 0.0001). The cropped blots are used in the figure, and the full-length blots are presented in Supplementary Fig. S3. **(d)** Expression of MrLip1 and MrLip5 in various clinical isolates of *M. restricta* was assessed by western

blot analysis. Nitrocellulose membranes were also stained with CPTA as a loading control. The cropped blots of are used in the figure, and the scanned full-length blots are presented in Supplementary Fig. S4. All western blot analysis were repeated at least three times, and representative images were presented.

plasma membrane, implying that the copper transport system of this fungus is different from that of *S. cerevisiae*. Nevertheless, the downregulation of the *CTR3* homolog in ZPT-treated *M. restricta* suggested that cellular copper levels were indeed increased slightly in the cells and implied that the small increase of copper accumulation might also contribute to the growth inhibition by ZPT. Unlike the copper transport system, *M. restricta* possesses highly-conserved fungal zinc transport systems. We noticed significantly upregulated expression of the homolog of *S. cerevisiae* vacuolar zinc transporters *Zrc1* and *Cot1* in ZPT-treated *M. restricta* cells, suggesting an increase in cellular zinc levels in the fungus.

Our transcriptome analysis revealed that ZPT inhibits Fe-S cluster synthesis in *M. restricta*, a result similar to that obtained for ZPT-treated *S. cerevisiae* cells^{24,25}. Fe-S cluster synthesis is one of the main iron metabolic processes that occurs in mitochondria, and increases in cellular zinc levels in response to ZPT treatment might be the main cause of Fe-S cluster synthesis inhibition in *M. restricta*. We should note that, although the change was minimal, a small increase of cellular copper levels might also contribute to inhibits Fe-S cluster synthesis in the ZPT-treated *M. restricta* cells. Several previous studies have suggested that hyper-accumulation of cellular zinc causes mitochondrial dysfunction that is associated with the accumulation of reactive oxygen species in the organelle, which leads to a reduction in ATP production, because this accumulation interferes with glycolysis, tricarboxylic acid cycle, and electron transport chain^{37–39}. Our data showed differential expression of a number of genes involved in mitochondrial functions, including the activities of the TCA cycle and electron transport chain, as well as significantly reduced aconitase activity in ZPT-treated *M. restricta*. In general, fungal strains that are deficient in Fe-S cluster synthesis increase expression of the genes responsible for iron uptake in the plasma membrane to compensate for the iron metabolism deficiency^{40–42}. ZPT-treated *S. cerevisiae* cells also showed increased expression of *FET3*, a component of the high-affinity reductive iron uptake system in the plasma membrane. Interestingly, we found that components of this system such as an iron permease and a ferroxidase, which have been identified in other fungi such as *S. cerevisiae*, *Candida albicans*, *Cryptococcus neoformans*, and *Aspergillus fumigatus*, are largely missing in the genome of *M. restricta*. However, we found that *M. restricta* possesses the genes required for siderophore synthesis and observed that MRES_12755, a homolog of *A. fumigatus* *SIDA*, which encodes L-ornithine N⁵-oxygenase in the siderophore synthesis pathway⁴³, was upregulated in dose-dependent manner, supporting our hypothesis that Fe-S cluster synthesis was significantly distorted in *M. restricta* in response to ZPT.

Our study revealed that expression of *SOD2*, the gene encoding a manganese dependent mitochondrial superoxide dismutase, may be directly or indirectly inhibited by ZPT in *M. restricta*. The *SOD2* gene was one of the most strongly downregulated genes in ZPT-treated *M. restricta*, an observation that led us to speculate that the significant downregulation of *Sod2* may contribute to decreased Fe-S cluster synthesis and reduced aconitase activity in the fungus. We developed this hypothesis because a number of studies showed that mitochondrial reactive oxygen species were increased in a mutant lacking *SOD2*, and that *SOD2*-mutant became hypersensitive to oxidative stress^{44–46}. How ZPT triggers downregulation of *SOD2* is not yet clear. However, a connection between cellular zinc toxicity and heme synthesis in other fungi may explain this phenomenon. Zinc toxicity causes reduced heme production in *A. fumigatus*⁴⁷, and deficiency in heme synthesis significantly reduced *SOD2* transcript levels in *S. cerevisiae*²⁸. Therefore, we speculated that ZPT increased cellular zinc toxicity, which in turn reduced heme synthesis, followed by a reduction in *SOD2* transcription in ZPT-treated *M. restricta* cells. Although an additional study is required to test this hypothesis, we suppose that the increase in cellular zinc introduced by ZPT triggered significant downregulation of *SOD2*, which disrupted Fe-S cluster synthesis and led mitochondrial dysfunction in *M. restricta*.

A recent genome analysis revealed that almost all *Malassezia* species, including *M. restricta*, lack the fatty acid synthase gene in their genomes. Instead, they possess numerous genes encoding lipases that acquire fatty acids as a nutrient source from sebum on host skin^{48–50}. After hydrolysis of exogenous lipids in sebum by lipases secreted by *Malassezia*, free fatty acids (FFA) may be released and transported into the fungal cells, suggesting that lipases play essential roles in the physiology of the fungi. The increased levels of FFA because of these lipases on skin surfaces lead to abnormal functioning of epidermal keratinocytes, which causes skin irritation^{13,51,52}. Moreover, oleic acid, an FFA generated by extracellular lipases of *Malassezia*, has been shown to induce scalp flaking and skin irritation in susceptible subjects². Previously, we identified 12 lipase-encoding genes in the genome of *M. restricta* and found that, among these genes, MRES_03670 (*MrLIP5*) is expressed most frequently on the surfaces of scalps of patients with dandruff, suggesting the importance of this lipase in fungus-host interactions. The present study revealed that ZPT treatment downregulated four out of 12 lipase genes (MRES_03205 [*MrLIP1*], MRES_03670 [*MrLIP5*], MRES_04670 [*MrLIP3*], and MRES_16530) in a dose-dependent manner, suggesting that inhibition of lipase expression is one of the main mechanisms by which ZPT inhibits *M. restricta*. Downregulation of lipase genes observed in our transcriptome analysis was confirmed by western blot analysis, which showed a reduction in the levels of the corresponding lipases. Reduced expression of lipases in response to ZPT treatment was also observed in several other clinical isolates of *M. restricta*, indicating that inhibition of lipase expression is a common mechanism of ZPT action against *M. restricta*. We should note that downregulation of *MrLIP5* by ZPT is particularly important because of the possible involvement of the corresponding protein in skin surface pathogenesis²⁶. However, the upstream regulator that inhibits the expression of lipases in response to ZPT treatment still needs to be identified. Taken together, our results suggest that at least three inhibitory mechanisms are associated with the action of ZPT against *M. restricta*: (i) an increase in cellular zinc levels, (ii) inhibition of mitochondrial functions, and (iii) a decrease in lipase expression.

Methods

Strains and culture conditions. *M. restricta* KCTC 27522, KCTC 27524, KCTC 27527, KCTC 27539, and KCTC 27542 were clinically isolated in our previous study and used here, along with the type strain *M. restricta* CBS 7877^{53,54}. *Malassezia* strains were grown in Leeming and Notman agar (LNA) solid medium (0.5% glucose, 1% peptone, 0.01% yeast extract, 0.8% bile salt, 0.1% glycerol, 0.05% glycerol monostearate, 0.05% Tween 60, 1.2% agar, 0.5% whole fat cow milk, and 170 µg/mL chloramphenicol) at 34 °C for 3 days⁵⁵. *S. cerevisiae* W303 was grown in YPD medium (1% yeast extract, 2% peptone, and 2% glucose)⁵⁶.

Determination of the ZPT susceptibility of *M. restricta*. We used a previously reported method with modifications to determine the susceptibility of *M. restricta* KCTC 27527 to ZPT (Sigma, St. Louis, MO, USA)⁵⁷. Briefly, a stock solution of ZPT at a final concentration of 20 µM was prepared and used for the susceptibility assay. The stock solution was serially diluted 2-fold with LNA medium and introduced into the wells of a 24-well plate. *M. restricta* cells, pre-grown in LNA medium, were inoculated using a cotton swab into each well of the 24-well plate containing different concentration of ZPT and incubated at 34 °C for 3 days. Minimal inhibitory concentrations (MICs) were determined, based on the lowest concentration at which there was no visible growth of the cells compared to that in medium without ZPT. The susceptibility assay was independently performed at least four times.

Determination of intracellular metal content. Total intracellular zinc, copper, iron, and manganese levels were determined by inductively coupled plasma-atomic emission spectroscopy (ICP-AES). *M. restricta* KCTC 27527 cells were cultured for 3 days and transferred to fresh LNA medium containing ZPT (0, 5, 10, or 20 µM) at 34 °C for 6 h. Cells were harvested, washed with washing buffer (50 mM Tris-HCl [pH 6.5] and 10 mM ethylenediaminetetraacetic acid three times and lyophilized, as described in a previous report²⁵. The cell mass was digested with 5 mL of HNO₃ and 3 mL of H₂O₂ using a microwave digestion system, START D (Milestone, Sorisole, Italy), and an ICP-AES analysis was performed using an Optima 5300 DV system (PerkinElmer, Waltham, MA, USA). To measure the concentrations of metals in *S. cerevisiae* W303, we followed methods described by Reeder *et al.*²⁵.

RNA isolation and transcriptome analysis. *M. restricta* KCTC 27527 cells were cultured in LNA medium at 34 °C for 3 days and transferred to fresh LNA medium containing ZPT (0, 5, 10, or 20 µM). The cells were incubated at 34 °C for 6 h and harvested for RNA extraction. Total RNA was extracted using an RNeasy Mini Kit (Qiagen, Hilden, Germany) following the manufacturer's instructions. The quality of RNA was evaluated using an Agilent 2100 Bioanalyzer (Agilent Technologies, Santa Clara, CA, US). Libraries for RNA sequencing were prepared with a TruSeq Stranded mRNA Sample Prep Kit (Illumina, San Diego, CA, US), according to the manufacturer's protocol, and RNA sequencing was performed on an Illumina HiSeq platform to generate 100-bp paired-end reads. Quality-filtered reads were aligned to the reference-genome sequence using bowtie2 v2.2.1⁵⁸. Mapped reads were counted by feature Counts in Subread package v1.4.3⁵⁹, and the relative transcript abundance was trimmed mean of M-values (TMM)-normalized by edgeR⁶⁰. Differential expression of few key genes were selected and validated by qRT-PCR using primers listed in Supplementary Table S4 and a 7500 system (Applied Biosystems, Foster, CA, USA). The actin gene (MRES_06100) was used as a reference.

Aconitase assay. Aconitase activity was measured, as described previously⁶¹. Briefly, *M. restricta* KCTC 27527 cells were cultured in LNA medium at 34 °C for 3 days, transferred to fresh LNA medium, incubated with or without ZPT (20 and 40 µM) at 34 °C for 16 h, and then harvested. The cells were lysed with Triton-citrate lysis buffer containing 22.9 mM Tris-HCl pH 7.5, 36.6 mM KCl, 1% Triton X-100, 2 mM sodium citrate, 0.6 mM MnCl₂, 1 mM dithiothreitol, 1 mM phenylmethylsulfonyl fluoride, and a 1% protease inhibitor cocktail. The polyacrylamide gel used to assess aconitase activity comprised a separating gel containing 8% acrylamide, 132 mM Tris-base, 132 mM borate and 3.6 mM citrate, and a stacking gel containing 4% acrylamide, 67 mM Tris-base, 67 mM borate, and 3.6 mM citrate. The running buffer contained 192 mM glycine, 3.6 mM citrate, and 25 mM Tris-HCl (pH 8.3). A total of 20 µg of protein extract from each sample was separated by electrophoresis at 160 V and 4 °C for 2.5 h. The aconitase activity was visualized by staining the gel with 100 mM Tris-HCl (pH 8.0), 1 mM nicotinamide adenine dinucleotide phosphate, 5 mM MgCl₂, 2.5 mM *cis*-aconitic acid, 1.2 mM methylthiazolyldiphenyl-tetrazolium bromide, 0.3 mM phenazine methosulfate, and 5 U/mL isocitrate dehydrogenase in the dark at 37 °C for 20 min. To show equal loading of each sample, the same amount of protein extract on the nitrocellulose membrane was stained with copper phthalocyanine-3,4,4',4'''-tetrasulphonic acid tetrasodium (CPTA).

Protein extraction and western blot analysis. *M. restricta* strains were cultured in LNA medium at 34 °C for 3 days and transferred to fresh LNA medium with or without 5 µM of ZPT, Zn, or Cu. The cells were incubated at 34 °C for an additional 16 h, harvested, and suspended in cell lysis buffer containing 140 mM NaCl, 50 mM 4-(2-hydroxyethyl)-1-piperazineethanesulfonic acid-KOH (pH 7.5), 1 mM ethylenediaminetetraacetic acid, 1% Triton X-100, 0.1% Na-deoxycholate, and 1 mM phenylmethylsulfonyl fluoride⁶². Total proteins were extracted by adding 600 µL of glass beads (0.5 mm) and vortexing the solution for 3 min. The western blots were performed using anti-MrLip1 and anti-MrLip5 sera, produced in our previous study⁵³, as primary antibodies and goat anti-rabbit IgG-horseshoe peroxidase (Santa-Cruz Biotechnology, Dallas, TX, USA) as the secondary antibody.

Statistical analysis. Statistical analysis for differences between each sample were calculated using the GraphPad QuickCalcs Web site (<https://www.graphpad.com/quickcalcs/ttest1.cfm>) with unpaired t-tests. $p < 0.05$ was accepted to mean a statistically significant difference.

Data availability. The datasets generated and analyzed during the current study are available in the Gene Express Omnibus (GEO) repository, under the accession number GSE112036.

References

1. Turner, G. A., Hoptroff, M. & Harding, C. R. Stratum corneum dysfunction in dandruff. *Int J Cosmet Sci* **34**, 298–306, <https://doi.org/10.1111/j.1468-2494.2012.00723.x> (2012).
2. DeAngelis, Y. M. *et al.* Three etiologic facets of dandruff and seborrheic dermatitis: Malassezia fungi, sebaceous lipids, and individual sensitivity. *J Investig Dermatol Symp Proc* **10**, 295–297, <https://doi.org/10.1111/j.1087-0024.2005.10119.x> (2005).
3. Peter, R. U. & Richarz-Barthauer, U. Successful treatment and prophylaxis of scalp seborrheic dermatitis and dandruff with 2% ketoconazole shampoo: results of a multicentre, double-blind, placebo-controlled trial. *Br J Dermatol* **132**, 441–445 (1995).
4. Danby, F. W., Maddin, W. S., Margesson, L. J. & Rosenthal, D. A randomized, double-blind, placebo-controlled trial of ketoconazole 2% shampoo versus selenium sulfide 2.5% shampoo in the treatment of moderate to severe dandruff. *J Am Acad Dermatol* **29**, 1008–1012 (1993).
5. Pierard, G. E., Arrese, J. E. & Pierard-Franchimont, C. & P, D. E. D. Prolonged effects of antidandruff shampoos - time to recurrence of Malassezia ovalis colonization of skin. *Int J Cosmet Sci* **19**, 111–117, <https://doi.org/10.1046/j.1467-2494.1997.171706.x> (1997).
6. Findley, K. *et al.* Topographic diversity of fungal and bacterial communities in human skin. *Nature* **498**, 367–370, <https://doi.org/10.1038/nature12171> (2013).
7. Xu, Z. *et al.* Dandruff is associated with the conjoined interactions between host and microorganisms. *Scientific reports* **6** (2016).
8. Clavaud, C. *et al.* Dandruff is associated with disequilibrium in the proportion of the major bacterial and fungal populations colonizing the scalp. *PLoS One* **8**, e58203, <https://doi.org/10.1371/journal.pone.0058203> (2013).
9. Honnavar, P. *et al.* Malassezia arunalokei sp. nov., a Novel Yeast Species Isolated from Seborrheic Dermatitis Patients and Healthy Individuals from India. *J Clin Microbiol* **54**, 1826–1834, <https://doi.org/10.1128/JCM.00683-16> (2016).
10. Cabanes, F. J., Coutinho, S. D., Puig, L., Bragulat, M. R. & Castella, G. New lipid-dependent Malassezia species from parrots. *Rev Iberoam Micol* **33**, 92–99, <https://doi.org/10.1016/j.riam.2016.03.003> (2016).
11. Wang, L. L. *et al.* Characterization of the major bacterial-fungal populations colonizing dandruff scalps in Shanghai, China, shows microbial disequilibrium. *Exp Dermatol* **24**, 398–400, <https://doi.org/10.1111/exd.12684> (2015).
12. Park, T. *et al.* Collapse of human scalp microbiome network in dandruff and seborrheic dermatitis. *Exp Dermatol* **26**, 835–838, <https://doi.org/10.1111/exd.13293> (2017).
13. Ro, B. I. & Dawson, T. L. The role of sebaceous gland activity and scalp microfloral metabolism in the etiology of seborrheic dermatitis and dandruff. *J Investig Dermatol Symp Proc* **10**, 194–197, <https://doi.org/10.1111/j.1087-0024.2005.10104.x> (2005).
14. White, E. C. Bactericidal Filtrates from a Mold Culture. *Science* **92**, 127, <https://doi.org/10.1126/science.92.2380.127> (1940).
15. White, E. C. & Hill, J. H. Studies on Antibacterial Products Formed by Molds: I. Aspergillilic Acid, a Product of a Strain of Aspergillus Flavus. *J Bacteriol* **45**, 433–443 (1943).
16. Dutcher, J. D. & Wintersteiner, O. The Structure of Aspergillilic Acid. *Journal of Biological Chemistry* **155**, 359–360 (1944).
17. Pansy, F. E., Stander, H., Koerber, W. L. & Donovick, R. *In vitro* studies with 1-hydroxy-2(1H) pyridinethione. *Proc Soc Exp Biol Med* **82**, 122–124 (1953).
18. Schwartz, J. R., C. W. Cardin, & T. L. Dawson. In *Textbook of cosmetic dermatology* (ed R. Baran and H. I. Maibach) Ch. 12, 259–272 (Martin Dunitz, Ltd., 2004).
19. Roques, C., Brousse, S. & Panizzutti, C. *In vitro* antifungal efficacy of ciclopirox olamine alone and associated with zinc pyrithione compared to ketoconazole against Malassezia globosa and Malassezia restricta reference strains. *Mycopathologia* **162**, 395–400, <https://doi.org/10.1007/s11046-006-0075-0> (2006).
20. Turner, G. A. *et al.* Enhanced efficacy and sensory properties of an anti-dandruff shampoo containing zinc pyrithione and climbazole. *Int J Cosmet Sci* **35**, 78–83, <https://doi.org/10.1111/ics.12007> (2013).
21. Ermolayeva, E. & Sanders, D. Mechanism of pyrithione-induced membrane depolarization in Neurospora crassa. *Appl Environ Microbiol* **61**, 3385–3390 (1995).
22. Albert, A., Rees, C. W. & Tomlinson, A. J. The influence of chemical constitution on antibacterial activity. VIII. 2-Mercaptopyridine-N-oxide, and some general observations on metalbinding agents. *Br J Exp Pathol* **37**, 500–511 (1956).
23. Khattar, M. M., Salt, W. G. & Stretton, R. J. The influence of pyrithione on the growth of micro-organisms. *J Appl Bacteriol* **64**, 265–272 (1988).
24. Yasokawa, D. *et al.* DNA microarray analysis suggests that zinc pyrithione causes iron starvation to the yeast Saccharomyces cerevisiae. *J Biosci Bioeng* **109**, 479–486, <https://doi.org/10.1016/j.jbiosc.2009.10.025> (2010).
25. Reeder, N. L. *et al.* Zinc pyrithione inhibits yeast growth through copper influx and inactivation of iron-sulfur proteins. *Antimicrob Agents Chemother* **55**, 5753–5760, <https://doi.org/10.1128/AAC.00724-11> (2011).
26. Park, M., Cho, Y. J., Lee, Y. W. & Jung, W. H. Whole genome sequencing analysis of the cutaneous pathogenic yeast Malassezia restricta and identification of the major lipase expressed on the scalp of patients with dandruff. *Mycoses* **60**, 188–197, <https://doi.org/10.1111/myc.12586> (2017).
27. DeAngelis, Y. M. *et al.* Isolation and expression of a Malassezia globosa lipase gene, LIP1. *J Invest Dermatol* **127**, 2138–2146, <https://doi.org/10.1038/sj.jid.5700844> (2007).
28. Galiazzo, F. & Labbe-Bois, R. Regulation of Cu, Zn- and Mn-superoxide dismutase transcription in Saccharomyces cerevisiae. *FEBS Lett* **315**, 197–200 (1993).
29. Muhlenhoff, U. *et al.* Compartmentalization of iron between mitochondria and the cytosol and its regulation. *Eur J Cell Biol* **94**, 292–308, <https://doi.org/10.1016/j.ejcb.2015.05.003> (2015).
30. Dancis, A. *et al.* Molecular characterization of a copper transport protein in S. cerevisiae: an unexpected role for copper in iron transport. *Cell* **76**, 393–402 (1994).
31. Knight, S. A., Labbe, S., Kwon, L. F., Kosman, D. J. & Thiele, D. J. A widespread transposable element masks expression of a yeast copper transport gene. *Genes Dev* **10**, 1917–1929 (1996).
32. Ding, C. *et al.* The copper regulon of the human fungal pathogen Cryptococcus neoformans H99. *Mol Microbiol* **81**, 1560–1576, <https://doi.org/10.1111/j.1365-2958.2011.07794.x> (2011).
33. Waterman, S. R. *et al.* Role of a CUF1/CTR4 copper regulatory axis in the virulence of Cryptococcus neoformans. *J Clin Invest* **117**, 794–802, <https://doi.org/10.1172/JCI30006> (2007).
34. Portnoy, M. E., Schmidt, P. J., Rogers, R. S. & Culotta, V. C. Metal transporters that contribute copper to metallochaperones in Saccharomyces cerevisiae. *Mol Genet Genomics* **265**, 873–882 (2001).
35. MacDiarmid, C. W., Gaither, L. A. & Eide, D. Zinc transporters that regulate vacuolar zinc storage in Saccharomyces cerevisiae. *EMBO J* **19**, 2845–2855, <https://doi.org/10.1093/emboj/19.12.2845> (2000).
36. Lee, Y. W., Lee, S. Y., Lee, Y. & Jung, W. H. Evaluation of Expression of Lipases and Phospholipases of Malassezia restricta in Patients with Seborrheic Dermatitis. *Ann Dermatol* **25**, 310–314, <https://doi.org/10.5021/ad.2013.25.3.310> (2013).
37. Gazaryan, I. G. *et al.* Zinc is a potent inhibitor of thiol oxidoreductase activity and stimulates reactive oxygen species production by lipoamide dehydrogenase. *J Biol Chem* **277**, 10064–10072, <https://doi.org/10.1074/jbc.M108264200> (2002).
38. Dineley, K. E., Votyakova, T. V. & Reynolds, I. J. Zinc inhibition of cellular energy production: implications for mitochondria and neurodegeneration. *J Neurochem* **85**, 563–570 (2003).
39. Lemire, J., Mailloux, R. & Appanna, V. D. Zinc toxicity alters mitochondrial metabolism and leads to decreased ATP production in hepatocytes. *J Appl Toxicol* **28**, 175–182, <https://doi.org/10.1002/jat.1263> (2008).
40. Foury, F. & Talibi, D. Mitochondrial control of iron homeostasis. A genome wide analysis of gene expression in a yeast frataxin-deficient strain. *J Biol Chem* **276**, 7762–7768, <https://doi.org/10.1074/jbc.M005804200> (2001).

41. Kumanovics, A. *et al.* Identification of FRA1 and FRA2 as genes involved in regulating the yeast iron regulon in response to decreased mitochondrial iron-sulfur cluster synthesis. *J Biol Chem* **283**, 10276–10286, <https://doi.org/10.1074/jbc.M801160200> (2008).
42. Chen, O. S. *et al.* Transcription of the yeast iron regulon does not respond directly to iron but rather to iron-sulfur cluster biosynthesis. *J Biol Chem* **279**, 29513–29518, <https://doi.org/10.1074/jbc.M403209200> (2004).
43. Hissen, A. H., Wan, A. N., Warwas, M. L., Pinto, L. J. & Moore, M. M. The *Aspergillus fumigatus* siderophore biosynthetic gene *sidA*, encoding L-ornithine N5-oxygenase, is required for virulence. *Infect Immun* **73**, 5493–5503, <https://doi.org/10.1128/IAI.73.9.5493-5503.2005> (2005).
44. Longo, V. D., Liou, L. L., Valentine, J. S. & Gralla, E. B. Mitochondrial superoxide decreases yeast survival in stationary phase. *Arch Biochem Biophys* **365**, 131–142, <https://doi.org/10.1006/abbi.1999.1158> (1999).
45. van Loon, A. P., Pesold-Hurt, B. & Schatz, G. A yeast mutant lacking mitochondrial manganese-superoxide dismutase is hypersensitive to oxygen. *Proc Natl Acad Sci USA* **83**, 3820–3824 (1986).
46. Celotto, A. M., Liu, Z., Vandemark, A. P. & Palladino, M. J. A novel *Drosophila* SOD2 mutant demonstrates a role for mitochondrial ROS in neurodevelopment and disease. *Brain Behav* **2**, 424–434, <https://doi.org/10.1002/brb3.73> (2012).
47. Yasmin, S. *et al.* The interplay between iron and zinc metabolism in *Aspergillus fumigatus*. *Fungal Genet Biol* **46**, 707–713, <https://doi.org/10.1016/j.fgb.2009.05.003> (2009).
48. Gioti, A. *et al.* Genomic insights into the atopic eczema-associated skin commensal yeast *Malassezia sympodialis*. *MBio* **4**, e00572–00512, <https://doi.org/10.1128/mBio.00572-12> (2013).
49. Wu, G. *et al.* Genus-Wide Comparative Genomics of *Malassezia* Delineates Its Phylogeny, Physiology, and Niche Adaptation on Human Skin. *PLoS Genet* **11**, e1005614, <https://doi.org/10.1371/journal.pgen.1005614> (2015).
50. Xu, J. *et al.* Dandruff-associated *Malassezia* genomes reveal convergent and divergent virulence traits shared with plant and human fungal pathogens. *Proc Natl Acad Sci USA* **104**, 18730–18735, <https://doi.org/10.1073/pnas.0706756104> (2007).
51. Mao-Qiang, M., Elias, P. M. & Feingold, K. R. Fatty acids are required for epidermal permeability barrier function. *J Clin Invest* **92**, 791–798, <https://doi.org/10.1172/JCI116652> (1993).
52. Katsuta, Y., Iida, T., Inomata, S. & Denda, M. Unsaturated fatty acids induce calcium influx into keratinocytes and cause abnormal differentiation of epidermis. *J Invest Dermatol* **124**, 1008–1013, <https://doi.org/10.1111/j.0022-202X.2005.23682.x> (2005).
53. Park, M., Jung, W. H., Han, S. H., Lee, Y. H. & Lee, Y. W. Characterisation and Expression Analysis of MrLip1, a Class 3 Family Lipase of *Malassezia restricta*. *Mycoses* **58**, 671–678, <https://doi.org/10.1111/myc.12412> (2015).
54. Guillot, J. & Gueho, E. The diversity of *Malassezia* yeasts confirmed by rRNA sequence and nuclear DNA comparisons. *Antonie Van Leeuwenhoek* **67**, 297–314 (1995).
55. Leeming, J. P. & Notman, F. H. Improved methods for isolation and enumeration of *Malassezia furfur* from human skin. *J Clin Microbiol* **25**, 2017–2019 (1987).
56. Thomas, B. J. & Rothstein, R. Elevated recombination rates in transcriptionally active DNA. *Cell* **56**, 619–630 (1989).
57. Sugita, T. *et al.* Antifungal activities of tacrolimus and azole agents against the eleven currently accepted *Malassezia* species. *J Clin Microbiol* **43**, 2824–2829, <https://doi.org/10.1128/JCM.43.6.2824-2829.2005> (2005).
58. Langmead, B. & Salzberg, S. L. Fast gapped-read alignment with Bowtie 2. *Nat Methods* **9**, 357–359, <https://doi.org/10.1038/nmeth.1923> (2012).
59. Liao, Y., Smyth, G. K. & Shi, W. The Subread aligner: fast, accurate and scalable read mapping by seed-and-vote. *Nucleic Acids Res* **41**, e108, <https://doi.org/10.1093/nar/gkt214> (2013).
60. Robinson, M. D., McCarthy, D. J. & Smyth, G. K. edgeR: a Bioconductor package for differential expression analysis of digital gene expression data. *Bioinformatics* **26**, 139–140, <https://doi.org/10.1093/bioinformatics/btp616> (2010).
61. Shi, Y., Ghosh, M. C., Tong, W. H. & Rouault, T. A. Human ISD11 is essential for both iron-sulfur cluster assembly and maintenance of normal cellular iron homeostasis. *Hum Mol Genet* **18**, 3014–3025, <https://doi.org/10.1093/hmg/ddp239> (2009).
62. Djordjevic, J. T., Del Poeta, M., Sorrell, T. C., Turner, K. M. & Wright, L. C. Secretion of cryptococcal phospholipase B1 (PLB1) is regulated by a glycosylphosphatidylinositol (GPI) anchor. *Biochem J* **389**, 803–812, <https://doi.org/10.1042/BJ20050063> (2005).

Acknowledgements

This study was supported by the Basic Science Research Program of the National Research Foundation of Korea (NRF), funded by the Ministry of Science, ICT, and Future Planning NRF-2016R1D1A1B03931890 (WHJ) and NRF-2016R1D1A1A09918488 (YWL).

Author Contributions

Park, Cho performed experiments. Park, Cho, Lee, Jung analyzed and interpreted data. Park, Cho, Lee, Jung wrote the manuscript text and prepared figures. All authors reviewed the manuscript.

Additional Information

Supplementary information accompanies this paper at <https://doi.org/10.1038/s41598-018-30588-2>.

Competing Interests: The authors declare no competing interests.

Publisher's note: Springer Nature remains neutral with regard to jurisdictional claims in published maps and institutional affiliations.



Open Access This article is licensed under a Creative Commons Attribution 4.0 International License, which permits use, sharing, adaptation, distribution and reproduction in any medium or format, as long as you give appropriate credit to the original author(s) and the source, provide a link to the Creative Commons license, and indicate if changes were made. The images or other third party material in this article are included in the article's Creative Commons license, unless indicated otherwise in a credit line to the material. If material is not included in the article's Creative Commons license and your intended use is not permitted by statutory regulation or exceeds the permitted use, you will need to obtain permission directly from the copyright holder. To view a copy of this license, visit <http://creativecommons.org/licenses/by/4.0/>.

© The Author(s) 2018